

#132 ASCE - Sym Dyn PROPERTIES of GRAVEL
SD-27 - San Diego, 95

PREDICTING LIQUEFACTION RESPONSE OF GRANULAR SOILS FROM PRESSUREMETER TESTS

by

Peter M. Byrne¹, Debasis Roy², Richard G. Campanella¹, and John Hughes³

ABSTRACT

Field and laboratory experience have shown that gravelly soils can liquefy during cyclic loading. Characterization of such a material either by direct tests of undisturbed samples or indirect means such as in-situ penetration testing is difficult because of the presence of large particles. In this paper an alternative approach involving back-analysis of in-situ pressuremeter test is proposed for obtaining the drained or skeleton behavior of the element. The undrained response is then predicted from the skeleton behavior by considering the volumetric constraint provided by the pore fluid.

Key elements of this procedure are: (a) use of a comprehensive but relatively simple numerical model that captures the drained or skeleton behavior of the material, (b) back analysis of a pressuremeter test to obtain the model parameters, (c) prediction of drained and undrained element response from the parameters obtained in step (b), and (d) validation by comparison with drained and undrained laboratory tests on undisturbed frozen samples.

INTRODUCTION

Occurrence of liquefaction in gravelly deposits during earthquakes have been documented in many case histories. Evans et al. (1992) give a list of case histories involving liquefaction of gravels. Laboratory testing of gravelly soils under undrained conditions simulating earthquake loading is difficult for two reasons: (a) it is very difficult to retrieve an undisturbed sample of gravelly soil; and (b) development of pore water pressure is usually underestimated for loose gravelly soils due to membrane compliance.

Drained as well as undrained stress-strain response of granular material is controlled by the skeleton, i.e., the effective stress tensor. The presence of water or other fluid in the pores serves merely as a volumetric constraint to the system. Thus, if the drained skeleton or element behavior can be captured in a stress-strain model, the undrained response can be predicted by incorporating the constraint due to the pore fluid. In this paper a simple elastic-

-
1. Professor, Department of Civil Engineering, University of British Columbia, Vancouver, B.C., Canada, V6T 1Z4
 2. Graduate Student, Department of Civil Engineering, University of British Columbia, Vancouver, B.C., Canada, V6T 1Z4.
 3. Hughes In-Situ Engineering Inc., 3009 S. Andrews Ave., North Vancouver.

plastic stress-strain model for simulating the drained or skeleton behavior of cohesionless soils is described. The corresponding undrained response can be inferred invoking appropriate volumetric constraint. The predicted behavior is then compared with laboratory measurements.

Estimates of the constitutive model parameters can be obtained from laboratory test data duly corrected for membrane compliance. Reliability of these values depends mainly upon sample disturbance and the accuracy with which the state of in-situ stress can be duplicated in the laboratory. Undisturbed samples of about 100 mm in diameter or smaller can be obtained from in-situ freezing although the technology is very expensive. However, testing of samples as large as 1 m in diameter and 2 m in height may be necessary due to the presence of particles of large size such as gravels. Facilities capable of handling such a large sample size are rare.

Alternatively, the parameters for the constitutive model can be estimated from inverse modeling of the in-situ cavity expansion test. The objective of the inverse modeling is to achieve a good fit between the model and the data by varying the model parameters. Once the model parameters giving a good fit have been obtained from drained loading, the undrained response can be predicted by applying a volumetric constraint.

Self boring pressuremeter tests have been successfully conducted at a location near Vancouver, B.C., in a predominately sandy soil with occasional gravels. One of these high quality tests have been analyzed in a following section to illustrate the procedure. Installation of a self boring pressuremeter becomes difficult in a soil comprising primarily of gravel size particles. In such a situation, however, in-situ cavity expansion data of a reasonable quality can be obtained from pre-bored pressuremeter tests. Given the difficulty in sampling and testing of gravelly soils in the laboratory, the approach of predicting soil behavior from in-situ cavity expansion test may form a rational basis for characterization of such a deposit in terms of their liquefaction potential.

THE STRESS-STRAIN MODEL

Both drained and undrained response of granular material are controlled by the skeleton behavior. The stress ratio, η , defined as the ratio of t and s , and the density have a significant influence on the shear response as shown in Fig. 1(a). Following Roscoe and Burland (1968), t and s are defined as $t = (\sigma_1' - \sigma_3')/2$ and $s = (\sigma_1' + \sigma_3')/2$, where σ_1' and σ_3' are the major and the minor principal stresses, respectively. Shear strains induce volumetric strains as shown in Fig. 1(b). Loose material is contractive when sheared to any effective stress ratio, while dense material is contractive for stress ratios below the $\eta = \sin \phi_{cv}$ line, where ϕ_{cv} is the constant volume angle of internal friction, and dilative above (Fig. 1(d)). This line is often referred to as the phase transformation line. Under very low confining stresses, loose material may exhibit dilative behavior at large strains. Unloading and

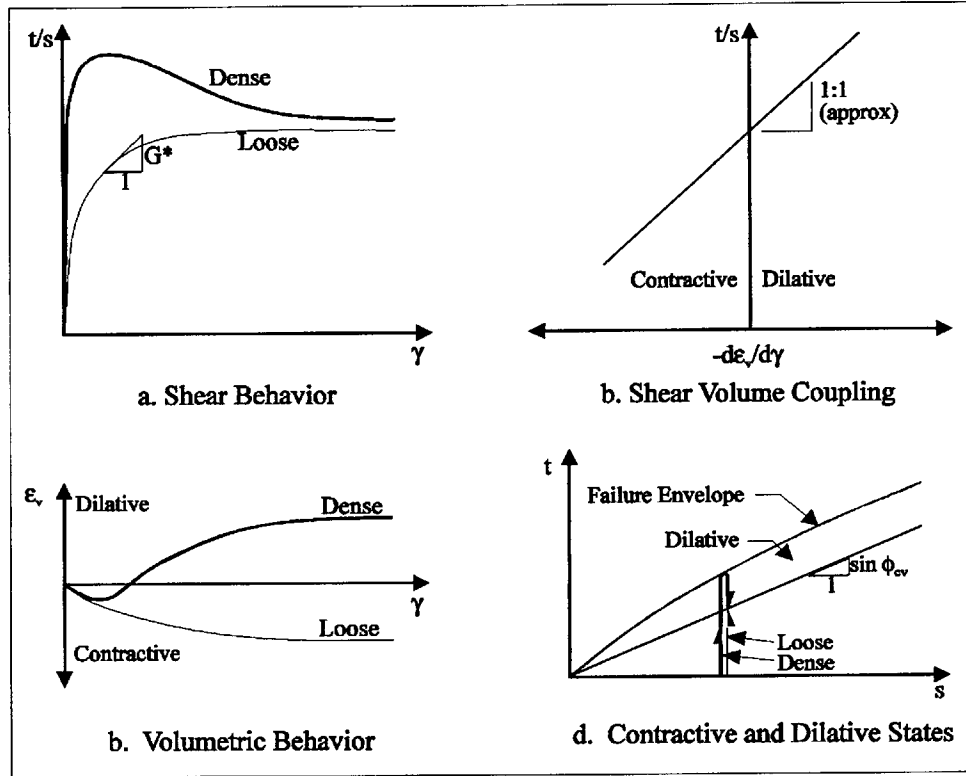


Fig. 1. Response of Granular Skeleton to Monotonic Shear Loading

reloading during shear would promote a stiff, essentially elastic response. Thus, a major portion of the observed strain during first loading is plastic rather than elastic. An elastic-plastic stress strain model used to simulate such a behavior is discussed below.

Elastic Properties

The elastic properties are assumed to be isotropic and modeled by two stress level dependent moduli: the shear modulus, G_e , and the bulk modulus, B_e . G_e and B_e are given by

$$G_e = K_g^e \times P_a \times (s/P_a)^{n_e} \quad (1)$$

where

K_g^e = the shear modulus number,

n_e = the shear modulus exponent,

P_a = the atmospheric pressure in the units stated, and

$$B_e = K_b^e \times P_a \times (s/P_a)^{m_e} \quad (2)$$

where

K_b^e = the shear modulus number and
 m_e = the shear modulus exponent.

The values of the parameters K_g^e , K_b^e , n_e and m_e can be obtained from unloading tests. Alternatively, supplementary seismic data can be used for their estimation. Based on available data, approximate values of K_g^e for loose, medium and dense granular materials are 300, 600 and 1200, respectively. In the absence of other information, the elastic bulk modulus number can be assumed to be equal to K_g^e . This amounts to a Poisson's ratio of 0.15 which lies in the range of 0.11 to 0.23 deemed appropriate for granular materials (Hardin, 1978). The elastic exponents n_e and m_e are approximately equal to 0.5.

Plastic Properties

Plastic strains are assumed to be caused by an increase in the absolute value of the stress ratio. Consequently, in terms of plasticity theory, lines of constant stress ratios become the yield loci of the model. The magnitude of the plastic shear strain on the plane of maximum shear stress, γ^p , is obtained by assuming a hyperbolic relationship between η and γ^p . This leads to the following expression for the tangent plastic modulus, G_p .

$$G_p = K_g^p P_a \left(\frac{s}{P_a} \right)^{n_p} \left(1 - R_f \frac{\eta}{\eta_f} \right)^2 \quad (3)$$

where

K_g^p = the plastic shear modulus number,
 n_p = the plastic shear modulus exponent (range: 0.25 to 1.0),
 η = the stress ratio on the plane of maximum shear stress,
 η_f = the stress ratio at failure,
 $R_f = \eta/\eta_{ult}$ (range: 0.5 to 1.0) and
 η_{ult} = the maximum stress ratio from the best fit hyperbola.

Smaller values of R_f are appropriate for denser deposits (Duncan et al., 1980; and Byrne et al., 1987). The approach described in the preceding paragraphs is similar to Duncan and Chang (1970), except that solely plastic strains rather than a combination of elastic and plastic strains are considered. The plastic shear modulus number, K_g^p , can vary from a low value of about 100 for a very loose material to about 4000 for a dense material. An increment of plastic shear strain, $d\gamma^p$, due to an increase in stress ratio, $d\eta$, during a monotonic loading is given by (see Fig. 1(a))

$$d\gamma^p = \frac{d\eta}{G^*} = \frac{d\eta}{G_p/s} \quad (4)$$

Since $\eta = t/s$,

$$d\eta = (dt/s) - t ds/s^2 \quad (5)$$

Hence,

$$d\gamma^p = \{ dt - (t/s)ds \} / G_p \quad (6)$$

An increase in stress ratio can be brought about by an increase in shear stress or a decrease in normal effective stress. Equation (6) shows that either change will cause an increment in plastic shear strain, $d\gamma^p$. If $ds = 0$, as in a drained simple shear test, the usual definition of G_p is obtained. If $dt = 0$, then a reduction in normal effective stress will cause a plastic shear strain increment, $d\gamma^p$, as shown in Fig. 2. For undrained tests, in which a significant pore water pressure rise occurs, ds will be negative. This will lead to an appreciable increase in plastic shear strain. Positive values of ds in Eqn.(6) are neglected. The second term inside the bracket in Eqn.(6) is a key feature of the formulation and is not generally considered in constitutive modeling of granular materials. In terms of classical plasticity, Eqn.(6) gives the hardening rule of this formulation.

The plastic volumetric strain increment, $d\epsilon_v^p$, can now be evaluated following energy considerations (Taylor, 1949) assuming dissipation of the plastic work increment to be solely in friction against the plastic shear strain increment:

$$d\epsilon_v^p = d\gamma^p (\sin \phi_{cv} - t/s) = d\gamma^p \times D_t \quad (7)$$

The term D_t controls the shear induced volumetric contraction or dilation. Contraction occurs at stress ratios less than $\sin \phi_{cv}$ and dilation at higher stress ratios. Eqn.(7) gives the non-associative flow rule of the formulation. Since planes of principal effective stress and strain increment coincide, the normal plastic strain, $d\epsilon_n^p$, on the plane of maximum shear is half the plastic volumetric strain $d\epsilon_v^p$. Hence from Eqn.(6) and Eqn.(7), the plastic stress-strain relationship on the plane of maximum shear is given by

$$\begin{Bmatrix} d\epsilon_n^p \\ d\gamma^p \end{Bmatrix} = \frac{1}{G_p} \begin{bmatrix} -tD_t/(2s) & (D_t/2) \\ (-t/s) & 1 \end{bmatrix} \begin{Bmatrix} ds \\ dt \end{Bmatrix} \quad (8)$$

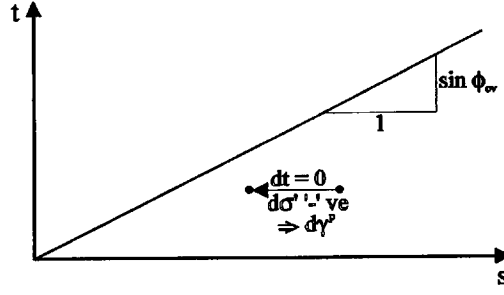


Fig. 2. Strain Increment due to Reduction in Normal Effective Stress

In general, the direction of the mobilized plane does not coincide with the reference coordinate system and the stress-strain relationship is transformed assuming coaxiality of plastic principal strain increments and the corresponding principal effective stresses into

$$\begin{Bmatrix} d\epsilon_x^p \\ d\epsilon_y^p \\ d\gamma_{xy}^p \end{Bmatrix} = [C_p] \begin{Bmatrix} d\sigma'_x \\ d\sigma'_y \\ d\tau_{xy} \end{Bmatrix} \quad (9)$$

where

- $d\epsilon_x^p$ = increment in plastic normal strain in the coordinate x direction,
- $d\epsilon_y^p$ = increment in plastic normal strain in the coordinate y direction,
- $d\gamma_{xy}^p$ = increment in plastic shear strain in the xy plane,
- $d\sigma'_x$ = increment in effective normal stress in the coordinate x direction,
- $d\sigma'_y$ = increment in effective normal stress in the coordinate y direction,
- $d\tau_{xy}$ = increment in shear stress in the xy plane, and
- $[C_p]$ = plastic compliance matrix.

The elastic and plastic strains are then added and the elasto-plastic compliance matrix is inverted to give the effective stress increment tensor, $\{d\sigma'\}$, in terms of the strain increments. This relationship describes the effective stress-strain response of the soil skeleton under drained loading.

$$\{d\sigma'\} = \begin{Bmatrix} d\sigma'_x \\ d\sigma'_y \\ d\tau_{xy} \end{Bmatrix} = [D_{ep}] \begin{Bmatrix} d\epsilon_x \\ d\epsilon_y \\ d\gamma_{xy} \end{Bmatrix} = [D_{ep}] \{d\epsilon\} \quad (10)$$

where

$d\epsilon_x = d\epsilon_x^p + d\epsilon_x^e$ = increment in normal strain in the coordinate x direction,
 $d\epsilon_y = d\epsilon_y^p + d\epsilon_y^e$ = increment in normal strain in the coordinate y direction,
 $d\gamma_{xy} = d\gamma_{xy}^p + d\gamma_{xy}^e$ = increment in shear strain in the xy plane,
 $d\epsilon_x^e$ = increment in elastic normal strain in the coordinate x direction,
 $d\epsilon_y^e$ = increment in elastic normal strain in the coordinate y direction,
 $d\gamma_{xy}^e$ = increment in elastic shear strain in the xy plane, and
 $[D_{ep}]$ = elasto-plastic element stiffness matrix in terms of effective stresses.

Undrained Response

In an undrained condition, volume compatibility requires that the volumetric strain of the soil skeleton, $d\epsilon_v$, must be equal to the volumetric strain of the fluid, $d\epsilon_v^f$. Thus:

$$d\epsilon_v^f = d\epsilon_v = d\epsilon_x + d\epsilon_y = [1 \ 1 \ 0] \{d\epsilon\} \quad (11)$$

The corresponding increment of pore fluid pressure, du , is given by

$$du = (B_f/n) d\epsilon_v^f = \frac{B_f}{n} [1 \ 1 \ 0] \{d\epsilon\} \quad (12)$$

where

B_f = the bulk modulus of the pore fluid, and
 n = the porosity of the skeleton.

Hence,

$$\begin{Bmatrix} du \\ du \\ 0 \end{Bmatrix} = \frac{B_f}{n} \begin{Bmatrix} 1 \\ 1 \\ 0 \end{Bmatrix} [1 \ 1 \ 0] \{d\epsilon\} = \frac{B_f}{n} \begin{bmatrix} 1 & 1 & 0 \\ 1 & 1 & 0 \\ 0 & 0 & 0 \end{bmatrix} \{d\epsilon\} = [D_f] \{d\epsilon\} \quad (13)$$

Since the total stress is the sum of the effective stress pore fluid pressure,

$$\{d\sigma\} = \{d\sigma'\} + \{du\} = [[D_{ep}] + [D_f]] \{d\epsilon\} \quad (14)$$

in which $[D_{ep}]$ and $[D_f]$ are the contributions of the skeleton and pore fluid to element stiffness, respectively; and $\{d\sigma\}$ is the incremental total stress tensor. The stress-strain relationship for the undrained conditions is thus obtained in terms of total stresses by adding the effective stress and pore fluid contributions to stiffness.

PROCEDURE FOR NUMERICAL ANALYSIS

In general, stress deformation response is governed by the laws of mechanics which require that equilibrium and compatibility be satisfied for the given boundary conditions and the appropriate stress-strain relationship. Finite element or finite difference techniques are routinely used to reasonably satisfy these conditions.

Here the analyses were carried out using the computer code FLAC (Fast Lagrangian Analysis of Continua) version 3.2 (Cundall, 1993). The program uses a finite difference technique. The domain is discretized into a quadrilateral grid in which each zone or element comprises of four triangles. The stiffness contribution of each zone is essentially the same as if it were represented by four constant strain triangular elements. Dynamic equilibrium, rather than static equilibrium, is satisfied using a step-by-step explicit time domain procedure. Large strains and displacements are accommodated by upgrading the nodal coordinates.

This approach has the advantage that the solution is numerically stable even when the problem is not statically stable. In this way, development of large strains and displacements prior to failure can be examined. The code allows the users to input their specific stress-strain model. The modified Matsuoka model (after Matsuoka and Nakai, 1977), as described in the previous section, was used for the analyses described hereafter.

Numerical Simulation of a Single Element Test

Simple shear or plane strain compression or extension tests can be modeled using a single zone or element with the appropriate initial stress state and boundary conditions. The characteristic drained or skeleton shear and volumetric response is simulated by neglecting the contribution of pore fluid to the element stiffness by setting $[D_f]$ to zero.

The undrained monotonic response of medium dense gravel samples tested under triaxial compression loading are shown in Fig. 3. The samples had relative densities of 23 and 54 % after consolidation to an isotropic state of 150 kPa stress. The predictions corresponding to plane strain rather than triaxial loading are also shown in Fig. 3 together with the values of the model parameters. The model was fitted to the data by adjusting the values of the parameters by trial and error.

Except for a slight over-estimation of pore water pressure at small strain, the model successfully captured both deviatoric and volumetric response of the samples. The difference between the triaxial and plane strain conditions and membrane compliance effects in the data may have affected the quality of the simulation. As a consequence, these results are of limited practical value. The purpose here was only to show that the model can capture the undrained response of gravel.

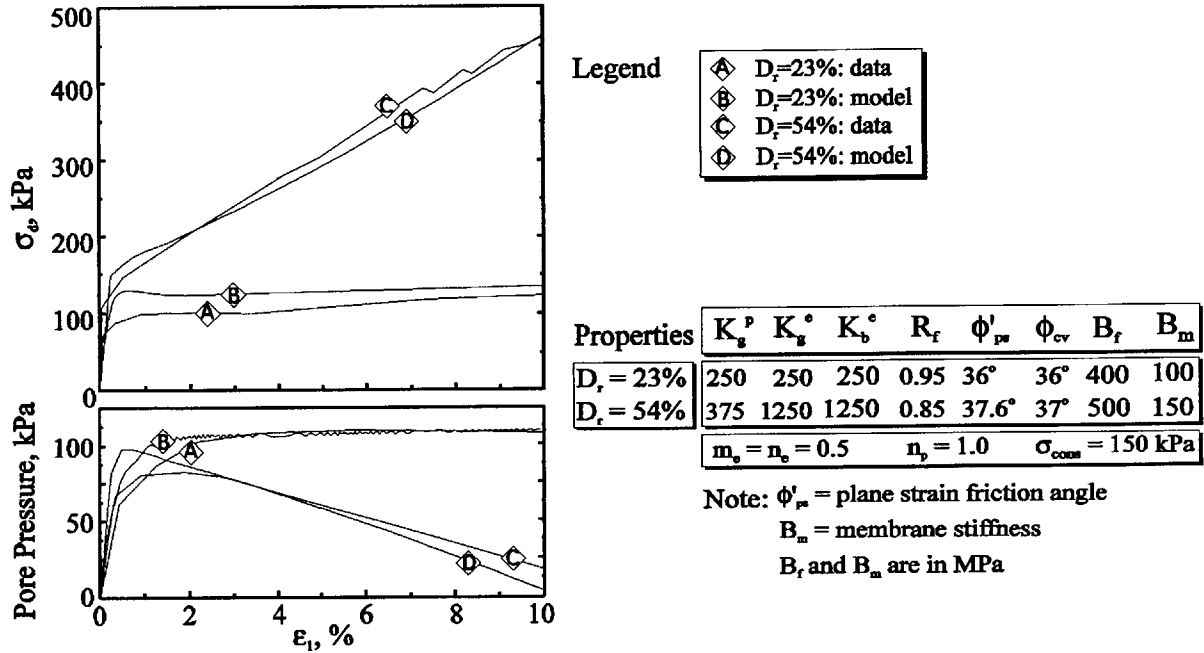


Fig. 3. Simulation of Triaxial Tests on Keenlyside Gravel

Inverse Modeling of Pressuremeter Tests

An in-situ cavity expansion test can be performed by installing a cylindrical probe - the self-boring pressuremeter - in the layer of interest by jetting or drilling. The self-boring pressuremeter used at the University of British Columbia (UBC) bores into the ground using a jetting technique. The inflatable section of the probe is 74 mm in diameter and 450 mm in height (Fig. 4). After installation at the horizon of interest, the probe is inflated by air pressure. The radial deflection at the center of the cylindrical cavity is monitored using six strain arms together with the air pressure and ambient pore water pressure in the same horizon (Campanella et al., 1990).

Cavity expansion tests were carried out at two sites in the Fraser Delta, south of the city of Vancouver, B.C. The soil profile at Massey Tunnel (south) includes fairly clean sand between 6 and 22 m depth. The water table was at 4 m depth during the test. The stratigraphy at KIDD # 2 consists of sand with occasional gravel lenses between 6 and 21 m depth. The relative densities at these two locations are about 50 and 75 %, respectively, based on estimates from interpretation of nearby piezocone sounding data. The measured cavity expansion curves at these locations are as shown in Fig. 5 (light lines).

The domain comprising of the zone of influence of the pressuremeter was discretized as shown in Fig. 6 for the finite difference analysis using FLAC. Model parameters were

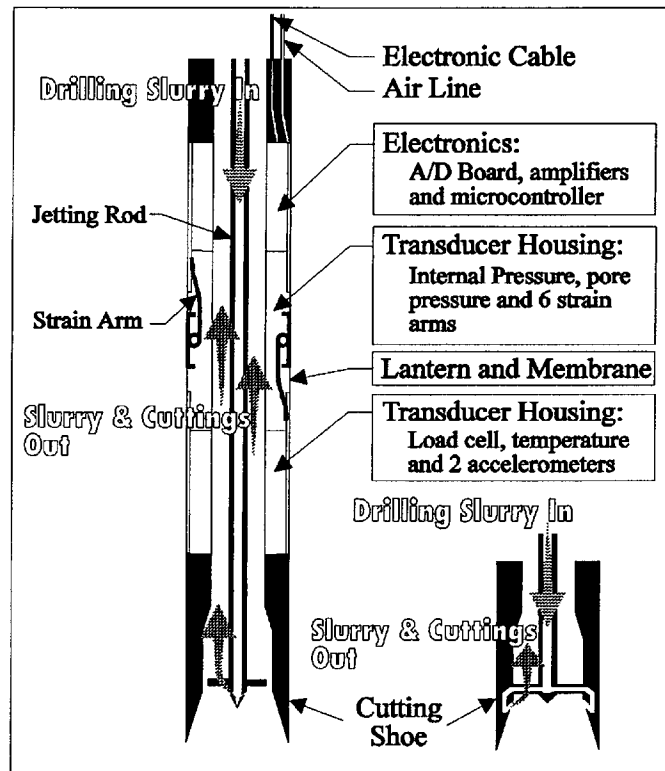


Fig. 4. Schematic Details of UBC Self Boring Pressuremeter

chosen and the face of the cavity was loaded in a strain controlled manner and the resulting radial stress at the face of the probe was computed (heavy lines in Fig. 5) and compared with the measured response. This process was repeated with slightly altered parameters until a reasonable fit was achieved between measurement and model prediction. The final best fit parameters obtained in this exercise are also listed in Fig. 5. The effective vertical and lateral stresses at KIDD # 2 was 110 and 60 kPa, respectively. The corresponding values for Massey Tunnel (south) were 125 and 60 kPa.

To examine the reliability of the procedure, expected pressuremeter responses for loose medium and dense granular materials corresponding to an effective vertical pressure of 100 kPa and $K_0 = 0.5$ were computed (Fig. 7). The large spread in response for the range of densities indicates that the problem of obtaining fundamental skeleton parameters from inverse modeling of cavity expansion data is reasonably well conditioned. Hence, the estimated soil skeleton behavior following this procedure can be considered reliable.

The feasibility of the self boring pressuremeter test for characterization of gravelly deposit should be carefully examined before its intended use. Experience suggests that the probes similar to those illustrated in Fig. 4 can be used in soils with occasional gravel sized particles. If the stratum contains a significant amount of gravels, the self boring technique

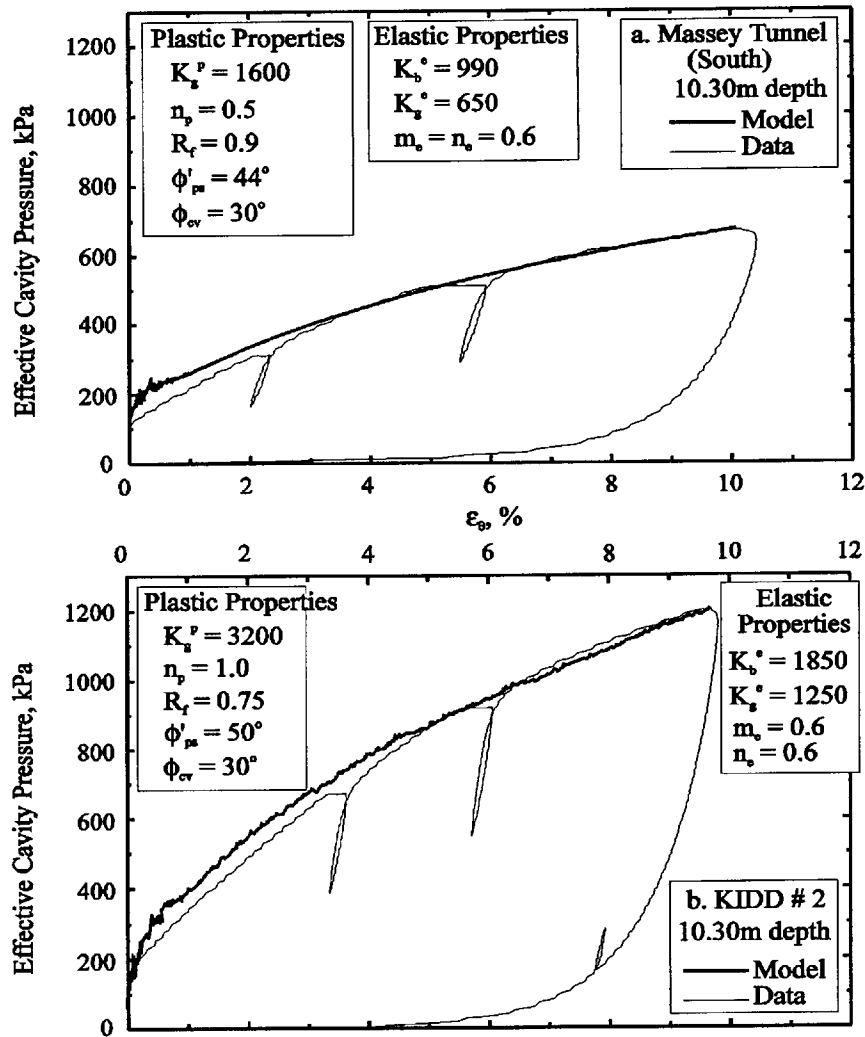


Fig. 5. Modeling of In-Situ Cavity Expansion Tests (ϵ_θ = Cavity Strain)

based on jetting does not appear to be effective. Under usual flow parameters (flow rate of about 30 liters per minute at approximately 350 kPa), the normal drilling slurry does not move the gravel sized particles from the layer of interest to the surface. This problem can be solved by performing cavity expansion tests in a pre bored hole. Cavity expansion data of a reasonable quality have been obtained from gravelly deposits using this technique recently.

Prediction of Element Response from Pressuremeter

The model parameters obtained from the pressuremeter test allow both drained and undrained element response to be computed. These predictions are shown in Fig. 8. The predicted undrained monotonic response is strain hardening for both materials and the residual

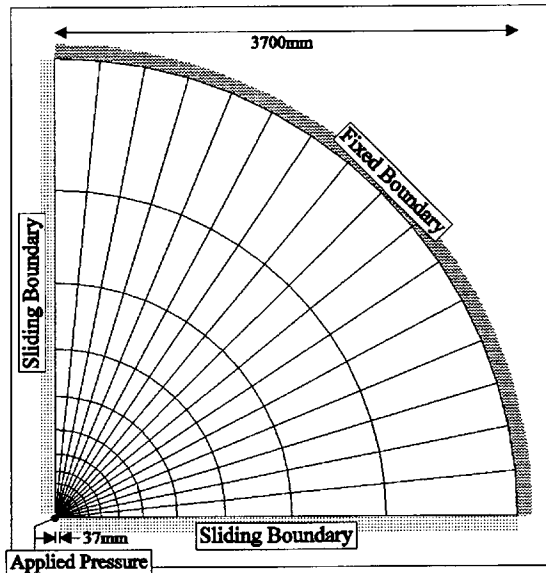


Fig. 6. Details of the Finite Difference Grid

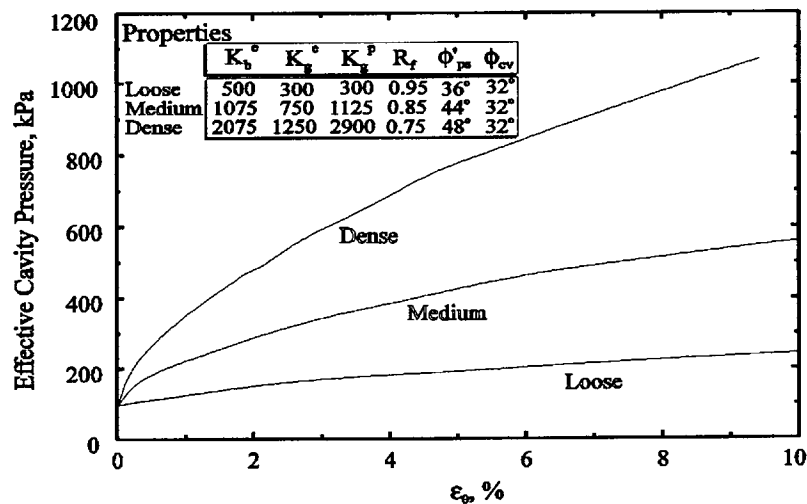


Fig. 7. Expected Pressure-Expansion Curves for Granular Soils at Different Densities

strengths are high. Frozen samples have been obtained near these locations and will be tested shortly. It will be of interest to compare these predictions with the measured laboratory response.

CONCLUSIONS

The stress-strain behavior of a soil element must be simulated accurately before attempting to predict the response of a soil-structure to applied loads. Once the element

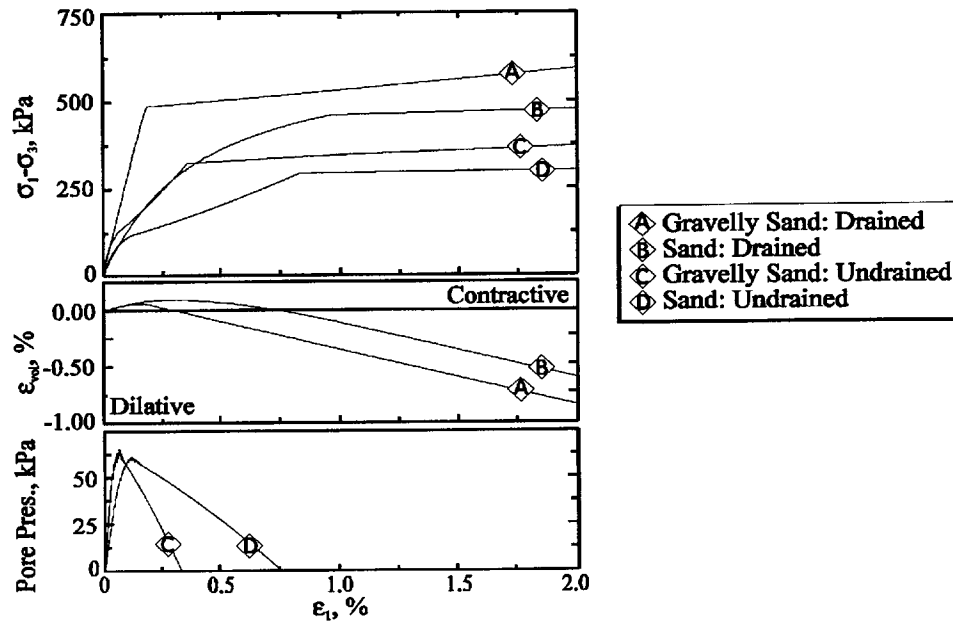


Fig. 8. Behavior of Plane Strain Element Predicted from In-situ Cavity Expansion Test

response is known, the soil structure can be modeled as a collection of such elements, and a finite element or difference technique can be used to assure that the elements deform in a compatible manner and equilibrium is generally satisfied. The element response is usually obtained from the recovery and testing of undisturbed samples, and its behavior is captured in a model that may range from simple elastic to complex elastic-plastic. Herein a reasonably simple elastic-plastic model is developed to simulate the skeleton behavior. The undrained behavior is inferred from the skeleton response by simply imposing a volumetric constraint governed by the compressibility of the pore fluid. It is shown that the undrained response of gravel samples under triaxial compression loading can be approximately simulated in this manner.

Because of the difficulty in retrieving and testing samples of granular material, particularly gravels, it is proposed that the fundamental skeleton behavior be obtained from inverse modeling of in-situ cavity expansion test employing a pressuremeter. Two pressuremeter tests in the Fraser Delta were back analyzed and the fundamental skeleton parameters were obtained. Based on these parameters, drained and undrained compression test results for a plane strain element were predicted. Frozen samples have been extracted from nearby locations and undrained tests will be performed on these samples shortly.

ACKNOWLEDGEMENTS

This study is partly funded by CANLEX (Canadian Liquefaction Experiment) - a collaborative project involving the National Science and Engineering Research Council of

Canada (NSERC), and several industrial collaborators. The authors would also like to thank the technicians, R.S. Jackson and H. Schrempp, for their help in performing the in-situ cavity expansion tests reported in this paper.

REFERENCES

- Byrne, P.M., Cheung, H., and Yan, L., "Soil Parameters for Deformation Analysis of Sand Masses," *Canadian Geotechnical Journal*, Vol. 24, No. 3, pp. 366-376, 1987.
- Campanella, R.G., Stewart, W.P., and Jackson, R.S., "Development of the UBC Self-Boring Pressuremeter," Proceedings, Third International Symposium on Pressuremeters, British Geotechnical Society, Oxford, pp. 65-72, 1990.
- Cundall, P.A., FLAC User's Manual, ITASCA Consulting Group, Inc., Minneapolis, 1993.
- Duncan, J.M., and Chang, C.Y., "Non-linear Analysis of Stress and Strain in Soils," *Journal of the Soil Mechanics and Foundation Engineering Division*, ASCE, Vol. 96, pp. 1629-1653, 1970.
- Duncan, J.M., Byrne, P., Wong, K.S., and Marby, P., "Strength, Stress-Strain and Bulk Modulus Parameters for Finite Element Analyses of Stresses and Movements in Soil Masses," Report No. UCB/GT/80-01, University of California, Berkeley, 70 p., 1980.
- Evans, M.D., Seed, H.B., and Seed, R.B., "Membrane Compliance and Liquefaction of Sluiced Gravel Specimens," *Journal of the Geotechnical Engineering Division*, ASCE, Vol. 118, No. GT6, pp. 856-872, 1992.
- Hardin, B.O., "Stress-Strain Behavior," *Earthquake Engineering and Soil Dynamics*, Proceedings, ASCE Geotechnical Engineering Division Specialty Conference, Pasadena, 1978, Vol. 1, pp. 3-90.
- Matsuoka, H., and Nakai, T., "Stress-Strain Relationship of Soil Based on S.M.P.," Proceedings, 9th International Conference on Soil Mechanics and Foundation Engineering, 1977, pp. 153-162.
- Roscoe, K.H., and Burland, J.B., "On The Generalised Stress-Strain Behaviour of 'Wet' Clay," in Engineering Plasticity, Heyman, J., and Leckie, F.A., Eds., Cambridge University Press, pp. 47-54, 1963.
- Taylor, D.W., Fundamental of Soil Mechanics, John Wiley and Sons, Inc., New York, 1948.